Immunity & Inflammation

BRIEF REPORT

Open Access

Fragrant TRPV3 agonists act as titratable organic adjuvants to amplify antigen-specific IgG response

Zhenglin Ji[1†], Ji Gao[1†], Yue Xin[2†], Cuifeng Li[1], Qianjin Lu[2,3*], Haijing Wu[2,4*] and Wanli Liu[1*]

Barrier epithelia are sensory interfaces that translate environmental cues into immune-instructive programs [1, 2]. In the skin, keratinocytes couple physical or chemical perturbations to rapid cytokine and chemokine release, thereby modulating antigen processing, antigen-presenting cell recruitment, and the efficacy of T cell help [2, 3]. In our previous studies, we identified farnesyl pyrophosphate (FPP), a mevalonate pathway metabolic intermediate, as an endogenous alarmin that enhances IgG antibody responses through keratinocyte-derived IL-6 and CCL20 (https://doi.org/10.1038/s41586-026-10167-6). In evolution, exogenous small molecules offer a complementary strategy in addition to endogenous alarmins to interrogate epidermal control of immunity: these exogenous compounds are chemically defined, readily titratable, and can be temporally constrained to probe causality.

Transient receptor potential vanilloid (TRPV3) is a Ca^{2+}-permeable ion channel enriched in keratinocytes and activated by multiple natural products, several of which are familiar odor-associated molecules produced in plant-derived organic compounds [4, 5]. Among these, Carvacrol (a phenolic monoterpenoid with an oregano-like aroma) and Camphor (a bicyclic monoterpene with a characteristic scent) are canonical TRPV3 agonists [6–8]. We sought to determine whether brief, localized engagement of TRPV3 by these fragrant ligands can act as an adjuvant-like trigger to amplify humoral immunity, and whether the resultant epidermal cytokine program is distinguishable from endogenous metabolite-driven signaling.

To test adjuvant-like activity, mice were co-immunized with a model protein antigen (OVA, 50 μg) and Carvacrol or Camphor over a dose range (4, 20, or 100 μg per mouse). ELISA analyses at days 7 and 14 revealed that both molecules increased OVA-specific IgG compared with antigen alone in a dose-dependent manner (Fig. 1a, b). Carvacrol at a dose of 100 μg used as an adjuvant showed no adverse effects on mouse body weight or survival (Supplementary Fig. 1a, b). The magnitude of enhancement was sustained into the later sampling point, consistent with an effect on developing humoral responses rather than a transient assay artifact.

We next examined early local signals that could connect epidermal activation to downstream antibody outcomes. One hour after local delivery, footpad tissues exhibited rapid induction of immune-relevant mediators. *Il6* and *Ccl20* were upregulated, accompanied by

†Zhenglin Ji, Ji Gao and Yue Xin these authors contributed equally to this work.

*Correspondence:
Qianjin Lu
qianlu5860@pumcderm.cams.cn
Haijing Wu
chriswu1010@csu.edu.cn
Wanli Liu
LiuLab@tsinghua.edu.cn
[1] State Key Laboratory of Membrane Biology, School of Life Sciences, Tsinghua-Peking Center for Life Sciences, Institute for Immunology, China Ministry of Education Key Laboratory of Protein Sciences, Tsinghua University, Beijing 100084, China
[2] Department of Dermatology, the Second Xiangya Hospital of Central South University, Hunan Key Laboratory of Medical Epigenomics, Changsha, Hunan 410011, China
[3] Institute of Dermatology, Chinese Academy of Medical Sciences and Peking Union Medical College, Nanjing 210042, China
[4] The Furong Laboratory, 87 Xiangya Road, Changsha, Hunan 410008, China

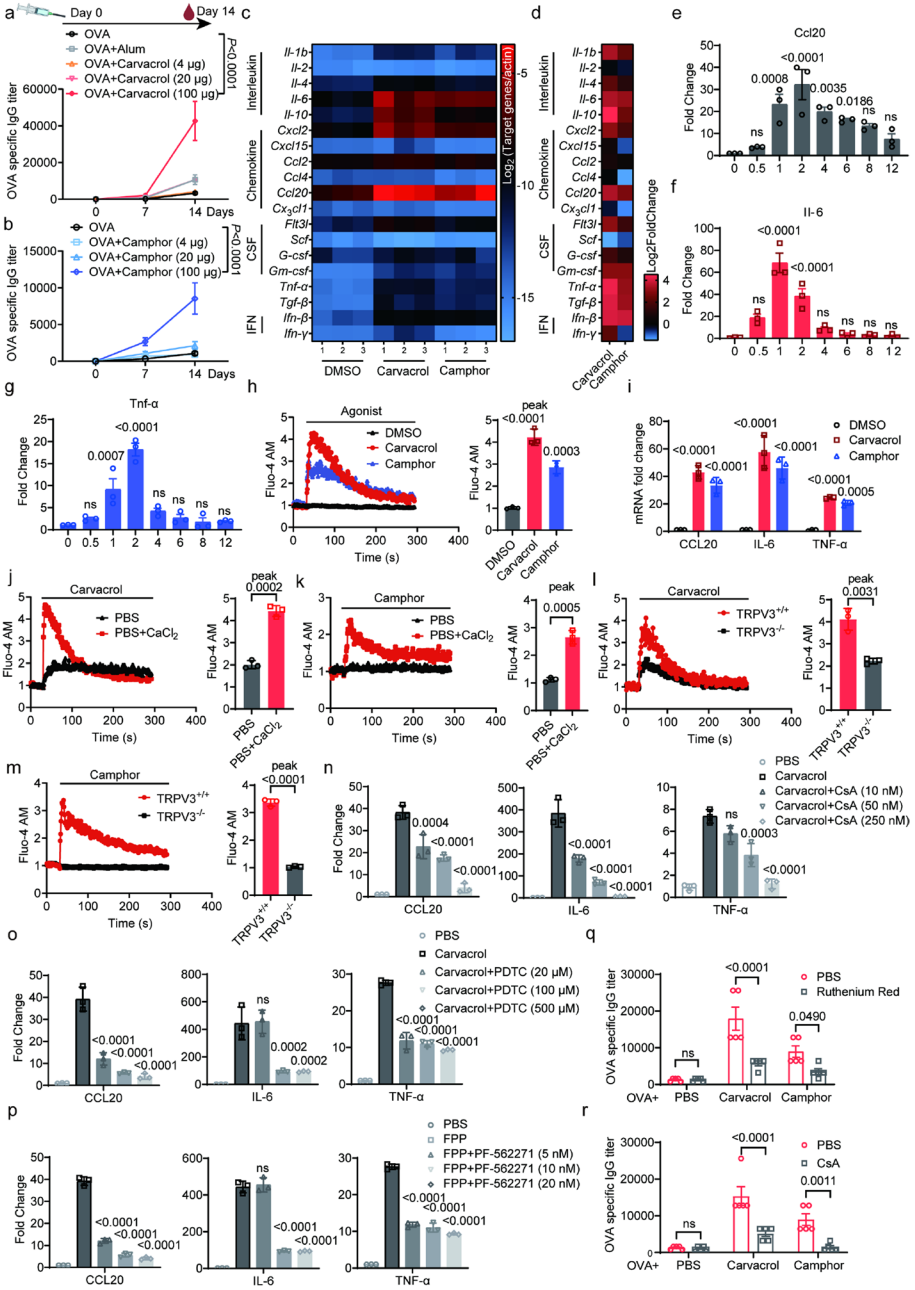

Fig. 1 Fragrant TRPV3 agonists enhance humoral responses and rapidly induce cytokine transcripts in skin. **a**, **b** OVA-specific IgG at days 7 and 14 following local co-immunization with OVA (50 μg) and Carvacrol or Camphor (4–100 μg) ($n = 3$, mean ± SEM). **c**, **d** Expression profiles from mice footpad tissue 1 h after Carvacrol or Camphor injection in comparison to PBS ($n = 3$, mean ± SEM). **e**–**g** Transcription levels of CCL20, IL-6 and TNF-α in mice footpad at indicated time points after Carvacrol injection ($n = 3$, mean ± SEM). **h** Relative changes in $[Ca^{2+}]_i$ over time in A431 cells loaded with the calcium indicator Fluo-4 AM and treated with 300 μM Carvacrol or 2 mM Camphor (black bar) were monitored by flow cytometry. Quantification of peak $[Ca^{2+}]_i$ after Carvacrol and Camphor stimulation ($n = 3$, mean ± SD). **i** Transcription levels of cytokines induced with Carvacrol or Camphor at different concentrations for 1 h in A431 cells. ($n = 3$, mean ± SD). **j**, **k** Addition of $CaCl_2$ to PBS buffer rescued $[Ca^{2+}]_i$ in A431 cells treated with 300 μM Carvacrol or 2 mM Camphor. Quantification of peak $[Ca^{2+}]_i$. ($n = 3$, mean ± SD). **l**, **m** Relative changes in $[Ca^{2+}]_i$ over time in WT and TRPV3-KO A431 cells loaded with the calcium indicator Fluo-4 AM and treated with 300 μM Carvacrol or 2 mM Camphor. Quantification of peak $[Ca^{2+}]_i$. ($n = 3$, mean ± SD). **n**-**p** Cytokine expression measured by qPCR in A431 cells after Carvacrol (300 μM) with indicated inhibitors ($n = 3$, mean ± SD). **q**, **r** Inhibitory effects of RR and CsA on Carvacrol and Camphor-enhanced expression of OVA-specific antibody ($n = 5$, mean ± SEM). Statistics computed by two-way ANOVA (**a**, **b**, **i**, **n**-**r**), one-way ANOVA (**e**–**g**), unpaired two-tailed t-test (**j**-**m**). ns, not significant. Data are representative of at least three independent experiments

induction of *Tnf* (Fig. 1c–g). These factors are linked to antigen-presenting cell recruitment and T cell help, consistent with a model in which brief epidermal stimulation creates a local environment permissive for efficient priming [9–15].

At the cellular level, we examined whether these results align with TRPV3-Ca^{2+} mechanism [7]. In A431 cells (a human epidermoid carcinoma cell line), loaded with Fluo-4, both Carvacrol and Camphor elicited increases in intracellular Ca^{2+} levels and cytokine expression (Fig. 1h, i). Interestingly, in A431 cells, Carvacrol upregulated the transcription of antibody promoting factors such as IL-6 and CCL20, while it exhibited no effect on the transcription of IL-18 (Supplementary Fig. 1c). Notably, Ca^{2+} entry required extracellular Ca^{2+}: Ca^{2+}-free conditions nearly abolished Carvacrol-evoked Ca^{2+} flux and eliminated Camphor-evoked flux, while re-addition of $CaCl_2$, but not $MgCl_2$, restored Ca^{2+} influx and rescued cytokine transcriptional outputs (Fig. 1j-k, Supplementary Fig. 1d-f).

To test receptor dependence, we examined TRPV3-deficient settings. TRPV3 loss markedly reduced agonist-driven Ca^{2+} influx (Fig. 1l, m) and attenuated cytokine induction (Supplementary Fig. 1g, h), supporting a causal TRPV3-Ca^{2+}-cytokine axis. We then investigated whether this epidermal Ca^{2+} signaling is required for the humoral endpoint in vivo. Co-immunization in the presence of ruthenium red (a TRP-channel blocker) or cyclosporin A (a calcineurin inhibitor) impaired Carvacrol/Camphor-mediated enhancement of OVA-specific IgG (Fig. 1n-r), linking receptor-proximal Ca^{2+} signaling and downstream Ca^{2+}-dependent pathways to antibody amplification. In intranasal immunization, Carvacrol exhibited adjuvant activity, whereas Camphor did not (Supplementary Fig. 1i).

These findings highlight an activation mode that is mechanistically separable from intracellular metabolite-binding routes. Prior structure-guided analyses have identified basic residues that support intracellular activation by pyrophosphate-containing metabolites; in contrast, exogenous agonists such as Carvacrol and Camphor can activate TRPV3 independently of those intracellular residues, consistent with preserved Ca^{2+} influx when TRPV3 variants defective for intracellular metabolite responsiveness are expressed (https://doi.org/10.1038/s41586-026-10167-6). This separation helps define a non-overlapping 'chemical sensory cue' module from an endogenous 'metabolic alarmin' module, and may provide a potential rationale for why fragrant agonists can produce an early cytokine mixture that includes *Tnf* in addition to *Il6* and *Ccl20* [7, 8].

More broadly, the TRP landscape of keratinocytes provides context for interpreting epidermal Ca^{2+} programs. For example, single-cell transcriptomic analyses of human (GSE179633 and GSE281449) [16, 17] and mouse skin [18] highlight TRPV3 among the highly expressed TRP family members in keratinocytes, alongside channels such as TRPM7, and multiple TRP channels are thermosensitive (Supplementary Fig. 2a-c). Besides the upregulation of TRPV3 in keratinocytes from patients with systemic lupus erythematosus (SLE) (https://doi.org/10.1038/s41586-026-10167-6), we found that its expression remained unchanged in atopic dermatitis (AD) patients and was significantly downregulated in those with psoriasis (Pso) patients, respectively (Supplementary Fig. 2d). TRPV3 is warm-sensitive with activation near physiological temperature, suggesting that temperature and chemical agonists may interact to shape epidermal Ca^{2+} dynamics and immune outputs. Agonist-evoked Ca^{2+} influx does not, however, affect TRPV3 transcription (Supplementary Fig. 2e). Building on these points, future work can systematically compare different TRP agonists and define how distinct epidermal cytokine compositions tune the magnitude and quality of germinal center and T follicular helper responses (Supplementary Fig. 2f).

At the barriers, skin infection activates the mevalonate (MVA) pathway in keratinocytes via the unfolded protein response (UPR) (https://doi.org/10.1038/s41586-026-10167-6). Notably, this infection-induced UPR response is distinctly different from those elicited by thapsigargin (TG), tunicamycin (TU), or ultraviolet (UV) treatment (Supplementary Fig. 3a). Furthermore, the activation of the UPR-MVA axis induced by infection is independent of TRPV3 (Supplementary Fig. 3b), and TG treatment can effectively activate the MVA pathway in HEK293 cells or human embryonic stem cells (hESCs) that either weakly express or lack TRPV3 expression (Supplementary Fig. 3c). Beyond the UPR, skin infection also elicits prominent apoptotic, reactive oxygen species (ROS)-mediated, and endoplasmic reticulum (ER) stress responses, reflecting the complexity of cellular stress cascades triggered by pathogenic invasion (Supplementary Fig. 3d-f). Thus, MVA activation in infection is UPR-dependent and TRPV3-independent, allowing orthogonal interrogation of epidermal immunity.

In parallel to these intracellular pathway activations, the functional consequences of skin infection on barrier immune responses were further characterized. Specifically, activation of the FPP-TRPV3 axis enhances antibody responses and recruits dendritic cells (DCs) to the infection site, while not affecting the activation status of skin-resident immune cells (https://doi.org/10.1038/s41586-026-10167-6). Notably, a significant reduction in total T cell numbers was observed at the infection site, whereas the proportions of $CD8^+$ T cells, Th1 cells, Th2

cells, and γδ Th17 cells remained unchanged (Supplementary Fig. 4a-e). This immune phenotypic feature was also validated in *Enterococcus faecalis* infections (Supplementary Fig. 4f-i), indicating its conservation across distinct bacterial pathogens. Furthermore, the chemokine CXCL12—critical for plasma cell recruitment—was downregulated in infected skin (Supplementary Fig. 4j), suggesting that plasma cells do not accumulate at the infection site at this time point.

Together, our data establish that two odor-associated TRPV3 agonists—Carvacrol and Camphor—function as tractable, titratable chemical adjuvants when delivered locally with protein antigen. Their effect is characterized by an IgG humoral amplification, a rapid *Il6/Ccl20/Tnf* epidermal transcriptional program, and a requirement for extracellular Ca^{2+}-dependent TRPV3 signaling and downstream calcineurin-sensitive pathways. These findings suggest that sensory-relevant chemicals can be leveraged to dissect and potentially engineer epidermis-centered immune potentiation modules that are experimentally separable from endogenous metabolite-driven alarmin routes.

Supplementary Information

The online version contains supplementary material available at https://doi.org/10.1007/s44466-026-00033-5.

Supplementary Material 1.

Supplementary Material 2.

Acknowledgements
We thank many colleagues for generously providing experimental materials and technical support. These include, but are not limited to, Prof. Bailong Xiao (Tsinghua University) for the TRPV3-KO mice; Peng Jiang (Tsinghua University) for A431 cell line; Prof. Jing-Ren Zhang (Tsinghua University) for Staphylococcus aureus; Dr. Xiaohui Liu from Metabolomics and Lipidomics Center and the Cell Biology Facility at Tsinghua University for LC-MS technique supports, and Dr. Ruiyu Gao for her assistance in animal experiments.

Authors' contributions
H.W., W.L., and Q.L. conceived and supervised the project. H.W. and W.L. designed experiments. Z.J., J.G., Y.X., and C.L. performed data acquisition, analysis, and interpretation under the supervision of H.W. and W.L., J.G. analyzed and interpreted the sequencing data. The initial draft of the manuscript was prepared by Z.J., J.G., Y.X., W.L. and H.W., with substantive revisions provided by all authors.

Funding
Wanli Liu is supported by grants from National Natural Science Foundation of China (32141004, 32430035, and 32441097), Shenzhen Medical Research Fund (C2404002 and B2402012), Ministry of Science and Technology of China Grants (2021YFC2302403) and Beijing Natural Science Foundation (Z230014). Qianjin Lu is supported by grants from National Key R&D Program of China (2022YFC3601800), the Major Program of the National Natural Science Foundation of China (82595960), the Key Program of National Natural Science Foundation of China (82430102), the Special Program of National Natural Science Foundation of China (NO. 32141004), the CAMS Innovation Fund for Medical Sciences (No.2021-I2M-1–059), and the Non-profit Central Research Institute Fund of Chinese Academy of Medical Sciences (2020-RC320-003). Haijing Wu is supported by grants from National Key R&D Program of China (2021YFC2702004), National Natural Science Foundation of China (82373448 and 82173425), the Major Scientific Research Program for High-Level Health Personnel in Hunan Province Health and Family Planning Commission (No.2023041), and the Hunan Provincial Natural Science Foundation Key Project (2025JJ30036). This study is also supported by research funds from Center for Life Sciences, Institute for Immunology at Tsinghua University.

Data availability
Data supporting the findings of this study are available from the corresponding author upon reasonable request.
For the S. aureus murine skin infection dataset, we downloaded publicly available scRNA-seq data from SRA database under accession no. PRJNA975496 [18]. For the *E. faecalis* murine skin infection dataset, we downloaded publicly available scRNA-seq data from GEO database under accession no. GSE229257 [19]. For the SLE and healthy control epidermis datasets, we downloaded publicly available scRNA-seq data from GEO database under accession no. GSE179633 and GSE281449 [16, 17]. For the UVB-treated healthy volunteer skin bulk RNA-seq dataset, we downloaded publicly available data from GEO database under accession no. GSE148535 [20]. For the TG-treated HEK293 cell and hESC bulk RNA-seq dataset, we downloaded publicly available data from GEO database under accession no. GSE293666 and GSE284753, respectively [21, 22]. For the psoriasis [23] and atopic dermatitis datasets [24], we downloaded publicly available data from the GEO database under accession numbers GSE162183 and GSE269981, respectively. The baseline expression data of TRPV3 in human cell types are obtained from Human Protein Atlas, www.proteinatlas.org [25, 26]. Further information and requests for resources and reagents should be firstly directed to the lead contact, W.L. (LiuLab@Tsinghua.edu.cn).

Declarations

Ethics approval and consent to participate
All experimental procedures involving animal experiments in this study were approved by the Institutional Animal Care and Use Committee (IACUC) of Tsinghua University, Beijing, China under assurance identification number, 15-LWL3 and 19-LWL1, respectively. All studies were conducted in strict accordance with governmental and institutional guidelines to ensure animal welfare.

Consent for publication
Not applicable.

Competing interests
The corresponding author Wanli Liu is a member of the Editorial Board of the journal Immunity & Inflammation. However, he was not involved in the peer review or decision-making process for this manuscript. The authors declare no other competing interests.

Received: 5 February 2026 Revised: 16 February 2026 Accepted: 19 February 2026
Published online: 05 March 2026

References

1. Kashem SW, Haniffa M, Kaplan DH. Antigen-presenting cells in the skin. Annu Rev Immunol. 2017;35:469–99.
2. Kabashima K, Honda T, Ginhoux F, et al. The immunological anatomy of the skin. Nat Rev Immunol. 2019;19:19–30.
3. Malissen B, Tamoutounour S, Henri S. The origins and functions of dendritic cells and macrophages in the skin. Nat Rev Immunol. 2014;14:417–28.
4. Fan J, Hu L, Yue Z, et al. Structural basis of TRPV3 inhibition by an antagonist. Nat Chem Biol. 2023;19:81–90.
5. Peier AM, Reeve AJ, Andersson DA, et al. A heat-sensitive TRP channel expressed in keratinocytes. Science. 2002;296:2046–9.
6. Broad L, Mogg A, Eberle E, et al. TRPV3 in drug development. Pharmaceuticals. 2016;9:55.

7. Szöllősi AG, Vasas N, Angyal Á, et al. Activation of TRPV3 regulates inflammatory actions of human epidermal keratinocytes. J Invest Dermatol. 2018;138:365–74.
8. Sherkheli MA, Vogt-Eisele AK, Weber K, et al. Camphor modulates TRPV3 cation channels activity by interacting with critical pore-region cysteine residues. Pak J Pharm Sci. 2013;26:431–8.
9. Sun X, Zhang H, Xu S, et al. Membrane-anchored CCL20 augments HIV Env-specific mucosal immune responses. Virol J. 2017;14:163.
10. Sierro F, Dubois B, Coste A, et al. Flagellin stimulation of intestinal epithelial cells triggers CCL20-mediated migration of dendritic cells. Proc Natl Acad Sci U S A. 2001;98:13722–7.
11. Kayamuro H, Abe Y, Yoshioka Y, et al. The use of a mutant TNF-α as a vaccine adjuvant for the induction of mucosal immune responses. Biomaterials. 2009;30:5869–76.
12. Gary EN, Tursi NJ, Warner B, et al. Mucosal chemokine adjuvant enhances synDNA vaccine-mediated responses to SARS-CoV-2 and provides heterologous protection in vivo. Cell Rep Med. 2022;3:100693.
13. Gary EN, Kutzler MA. Defensive driving: directing HIV-1 vaccine-induced humoral immunity to the mucosa with chemokine adjuvants. J Immunol Res. 2018;2018:1–14.
14. Dienz O, Eaton SM, Bond JP, et al. The induction of antibody production by IL-6 is indirectly mediated by IL-21 produced by CD4+ T cells. J Exp Med. 2009;206:69–78.
15. Su LK, Yu F, Li ZF, et al. Intranasal co-delivery of IL-6 gene enhances the immunogenicity of anti-caries DNA vaccine. Acta Pharmacol Sin. 2014;35:592–8.
16. Zheng M, Hu Z, Mei X, et al. Single-cell sequencing shows cellular heterogeneity of cutaneous lesions in lupus erythematosus. Nat Commun. 2022;13:7489.
17. Nakamizo S, Kabashima K, Morimoto N, et al. Single-Cell RNA Sequencing Reveals Age-Related Changes in Epidermal Cell Populations and Interactions. J Invest Dermatol. 2025;145:1502–5.
18. Qian X, Tong M, Zhang T, et al. IL-24 promotes atopic dermatitis-like inflammation through driving MRSA-induced allergic responses. Protein Cell. 2025;16:188–210.
19. Celik C, Lee STT, Tanoto FR, et al. Decoding the complexity of delayed wound healing following *Enterococcus faecalis* infection. Elife. 2024;13:RP95113.
20. Skopelja-Gardner S, An J, Tai J, et al. The early local and systemic type I interferon responses to ultraviolet B light exposure are cGAS dependent. Sci Rep. 2020;10:7908.
21. Sun J, Lee K, Kutseikin S, et al. Identification of a selective pharmacologic IRE1/XBP1s activator with enhanced tissue exposure. ACS Chem Biol. 2025;20:993–1003.
22. Traini L, Negueruela J, Elvira B, et al. Genome editing of TXNIP in human pluripotent stem cells for the generation of hepatocyte-like cells and insulin-producing islet-like aggregates. Stem Cell Res Ther. 2025;16:225.
23. Gao Y, Yao X, Zhai Y, et al. Single cell transcriptional zonation of human psoriasis skin identifies an alternative immunoregulatory axis conducted by skin resident cells. Cell Death Dis. 2021;12:450.
24. Chennareddy S, Rindler K, Meledathu S, et al. Single-cell RNA sequencing of chronic idiopathic erythroderma defines disease-specific markers. J Allergy Clin Immunol. 2025;155:892–908.
25. Karlsson M, Zhang C, Mear L, et al. A single-cell type transcriptomics map of human tissues. Sci Adv. 2021;7:eabh2169.
26. Uhlen M, Fagerberg L, Hallstrom BM, et al. Proteomics. Tissue-based map of the human proteome. Science. 2015;347:1260419.

Publisher's Note